Time propagation of constrained coupled Gaussian wave packets

Tomaž Fabčič,[a] Jörg Main, and Günter Wunner
Institut für Theoretische Physik 1, Universität Stuttgart, 70550 Stuttgart, Germany

(Received 21 June 2007; accepted 13 November 2007; published online 31 January 2008)

The dynamics of quantum systems can be approximated by the time propagation of Gaussian wave packets. Applying a time dependent variational principle, the time evolution of the parameters of the coupled Gaussian wave packets can be calculated from a set of ordinary differential equations. Unfortunately, the set of equations is ill behaved in most practical applications, depending on the number of propagated Gaussian wave packets, and methods for regularization are needed. We present a general method for regularization based on applying adequate nonholonomic inequality constraints to the evolution of the parameters, keeping the equations of motion well behaved. The power of the method is demonstrated for a nonintegrable system with two degrees of freedom.
 [DOI: 10.1063/1.2821751]

I. INTRODUCTION

The method of Gaussian wave packet propagation is a popular tool for quantum dynamics computations. Within this approximation it is assumed that an initially Gaussian wave packet (GWP) stays Gaussian for all times. The time evolution of the wave packet is given by the time evolution of its parameters like width, phase, center, and momentum.[1] For a single GWP, this rather crude approximation is in general only valid for short time propagation. The approximation can be significantly improved, if a superposition of GWPs is used and these GWPs are propagated in concert, since the number of adjustable parameters is increased and the overall wave function is no longer restricted to a Gaussian shape.[2–5] The equations of motion for the Gaussian parameters are obtained from a time dependent variational principle (TDVP). It is well known that these coupled equations of motion for the time dependent parameters become ill conditioned from time to time during the integration depending on how many GWPs are used. The reasons for the ill conditioned behavior of the differential equations are near singularities of a matrix that has to be inverted after each time step of integration.[3–7] Using step size control the time steps of the integration algorithm can become extremely small making the method impracticably slow. In the worst case even a failure of the numerical matrix inversion or the further integration may occur.

Different solutions to this numerical problem were proposed, e.g., a regularization based on a singular value decomposition.[7] The singular value decomposition is capable of regularizing the equations of motion in the sense that the method does not break down; however, it does not solve the problem with the tiny step sizes.[8] Another proposal is to adjust the number of GWPs during evolution by increasing or reducing their number depending on whether the wave function spreads or shrinks to avoid redundancy.[3,4,9]

It has also been discussed to simplify the equations of motion by keeping the widths of the propagated GWPs fixed, called frozen Gaussian approximation,[3–5,10] or much cruder, to neglect the coupling between the GWPs.[3,5] Another proposal is to reduce the variational freedom by forcing the GWPs to run on their classical trajectories.[2,6,11] But, of course, these grave restrictions severely reduce the accuracy of the GWP method.

Here, we present a novel method to overcome the numerical problems, or more precisely, a method that avoids numerical problems in the first place. The idea is to impose adequate nonholonomic inequality constraints to the motion of each GWP, keeping the matrix regular. These constraints only become active when it is numerically necessary and, otherwise, leave the full variational freedom of the trial function. The method presented here is general and allows for the application of arbitrary (inequality) constraints not only on GWP trial functions. There is numerical evidence that near matrix singularities usually result from widely varying amplitudes of largely overlapping GWPs. In our calculations it was sufficient to account for one ingredient of the matrix singularity only, i.e., to constrain the amplitudes of the individual GWPs to a reasonable domain. We account for the constraints in the time dependent variational principle and obtain different equations of motion as compared to the unconstrained variation. However, the equations of motion still have the form of a matrix equation as in the unconstrained case. Properly chosen constraints only slightly decrease the accuracy of the variational approximation. The additional error introduced by the constraints decreases with a growing number of GWPs. The method is able to avoid numerical problems rendering the integration by orders of magnitude faster.

The article is organized as follows. In Sec. II we recapitulate the time dependent variational principle. The equations of motion for the Gaussian parameters obtained from the TDVP applied to GWPs are given for completeness. In Sec. III we account for the inequality constraints in the TDVP and derive the regularized equations of motion. In Sec. IV we compare numerical results obtained from the GWP method with and without constraints in a two-

[a]Electronic mail: fabcic@itp1.uni-stuttgart.de.

dimensional (2D) nonintegrable model potential, namely, the 2D diamagnetic hydrogen atom. The accuracy of the constrained method is demonstrated by comparison with other propagation techniques. A summary is given in Sec. V.

II. TIME DEPENDENT VARIATIONAL PRINCIPLE

The evolution of a quantum mechanical wave function is determined by the Schrödinger equation,

$$i\dot{\psi}(t) = H\psi(t),$$

where the wave function $\psi(t)$ is an element of the Hilbert space. An approximate solution $\chi(t)$ on a given manifold in Hilbert space can be obtained by a TDVP.[12–15] Here, we choose the formulation of McLachlan,[14] or equivalently, the minimum error method,[3] where the norm of the deviation between the right and the left-hand sides of the Schrödinger equation with respect to the trial function is to be minimized. The quantity

$$I = \|i\dot{\phi}(t) - H\chi(t)\|^2 \overset{!}{=} \min$$

is to be varied with respect to ϕ only, and then $\dot{\chi} \equiv \dot{\phi}$ is chosen. We assume the approximation manifold to be parametrized by a set of time dependent parameters $\mathbf{z}(t) = (z_1(t), \ldots, z_{n_p}(t))$, i.e., $\chi(t) = \chi(\mathbf{z}(t))$. In terms of these parameters the quantity I reads

$$I = \left\langle \frac{\partial\chi}{\partial\mathbf{z}}\cdot\dot{\mathbf{z}} \middle| \frac{\partial\chi}{\partial\mathbf{z}}\cdot\dot{\mathbf{z}} \right\rangle - i\left\langle H\chi \middle| \frac{\partial\chi}{\partial\mathbf{z}}\cdot\dot{\mathbf{z}} \right\rangle + i\left\langle \frac{\partial\chi}{\partial\mathbf{z}}\cdot\dot{\mathbf{z}} \middle| H\chi \right\rangle + \langle H\chi|H\chi\rangle, \tag{1}$$

which is a quadratic function of $\dot{\mathbf{z}}$ for fixed values of $\mathbf{z}$. The variation $\delta\phi$ carries over to variations $\delta\dot{\mathbf{z}}$ leading to the condition

$$\frac{\partial I}{\partial \dot{z}_j} = 0, \quad j = 1, \ldots, n_p. \tag{2}$$

For complex parameters $z_j = z_{jr} + iz_{ji}$, one has the freedom to take either $\partial I/\partial \dot{z}_{jr} = 0$ and $\partial I/\partial \dot{z}_{ji} = 0$ or to treat $\dot{z}_j^*$ and $\dot{z}_j$ formally as independent parameters and to take either $\partial I/\partial \dot{z}_j = 0$ or $\partial I/\partial \dot{z}_j^* = 0$. The resulting equations of motion are equivalent and read

$$K\dot{\mathbf{z}} = -i\mathbf{h}, \tag{3}$$

in case of complex parameters $\mathbf{z}$, where

$$K = \left\langle \frac{\partial\chi}{\partial\mathbf{z}} \middle| \frac{\partial\chi}{\partial\mathbf{z}} \right\rangle, \quad \mathbf{h} = \left\langle \frac{\partial\chi}{\partial\mathbf{z}} \middle| H|\chi \right\rangle. \tag{4}$$

The Hermitian matrix K is positive semidefinite since

$$\mathbf{c}^\dagger \left\langle \frac{\partial\chi}{\partial\mathbf{z}} \middle| \frac{\partial\chi}{\partial\mathbf{z}} \right\rangle \mathbf{c} = \left\langle \frac{\partial\chi}{\partial\mathbf{z}}\cdot\mathbf{c} \middle| \frac{\partial\chi}{\partial\mathbf{z}}\cdot\mathbf{c} \right\rangle = \left\| \frac{\partial\chi}{\partial\mathbf{z}}\cdot\mathbf{c} \right\|^2 \geqslant 0, \quad \forall\, \mathbf{c} \in \mathbb{C}^{n_p}, \tag{5}$$

ensuring that the extremum of the quadratic quantity I is a minimum.

The Schrödinger equation is replaced by a system of ordinary first order differential equations of motion for the parameters $\mathbf{z}(t)$, where after every time step of integration the set of simultaneous linear equations (3) must be solved for the time derivatives $\dot{\mathbf{z}}$ if a numerical algorithm for ordinary differential equations, e.g., Runge-Kutta or Adams, is used.

A. Application of the TDVP to GWPs

In this article a superposition of GWP as trial function is discussed. Each GWP ($\mathbf{x} \in \mathbb{R}^D$) is of the form

$$g(\mathbf{y}^k, \mathbf{x}) = e^{i((\mathbf{x}-\mathbf{q}^k)A^k(\mathbf{x}-\mathbf{q}^k)+\mathbf{p}^k\cdot(\mathbf{x}-\mathbf{q}^k)+\gamma^k)}, \tag{6}$$

where A^k is a complex symmetric $D\times D$ matrix, the momenta $\mathbf{p}^k$ and centers $\mathbf{q}^k$ are real, D-dimensional vectors, and the phase and normalization are given by the complex scalars γ^k. The Gaussian parameters of the kth GWP are denoted by $\mathbf{y}^k = (A^k, \mathbf{p}^k, \mathbf{q}^k, \gamma^k)$. Their time argument is omitted for brevity. The trial function is a superposition of N such GWPs,

$$\chi(\mathbf{z}, \mathbf{x}) = \sum_{k=1}^{N} g(\mathbf{y}^k, \mathbf{x}), \quad \mathbf{z} = (\mathbf{y}^1, \ldots, \mathbf{y}^N). \tag{7}$$

Using a splitting of the Hamiltonian $H = T + V$, we obtain

$$\begin{aligned} i\dot{\chi} - T\chi = \sum_{k=1}^{N} \Big(&\Big[-\dot{\gamma}^k + i\,\mathrm{tr}\,A^k + \mathbf{p}^k\cdot\Big(\dot{\mathbf{q}}^k - \tfrac{1}{2}\mathbf{p}^k\Big)\Big] \\ &+ [-\dot{\mathbf{p}}^k + 2A^k(\dot{\mathbf{q}}^k - \mathbf{p}^k)]\cdot(\mathbf{x}-\mathbf{q}^k) + (\mathbf{x}-\mathbf{q}^k) \\ &\times[-\dot{A}^k - 2(A^k)^2](\mathbf{x}-\mathbf{q}^k)\Big) g(\mathbf{y}^k, \mathbf{x}) \\ \equiv \sum_{k=1}^{N} &\Big(v_0^k + \mathbf{v}_1^k\cdot\mathbf{x} + \tfrac{1}{2}\mathbf{x}V_2^k\mathbf{x}\Big) g(\mathbf{y}^k, \mathbf{x}), \end{aligned} \tag{8}$$

which defines, after sorting by powers of $\mathbf{x}$, the complex scalars v_0^k, the complex vectors $\mathbf{v}_1^k \in \mathbb{C}^D$, and the complex symmetric $D\times D$ matrices V_2^k as the coefficients of a second order polynomial. According to the TDVP these coefficients $(v_0^k, \mathbf{v}_1^k, V_2^k)$, $k = 1, \ldots, N$, are calculated from a set of linear equations,

$$\begin{aligned} &\sum_{k=1}^{N} v_0^k \langle g^l|x_i^m x_j^n|g^k\rangle + \sum_{k=1}^{N} \langle g^l|x_i^m x_j^n \mathbf{x}\cdot\mathbf{v}_1^k|g^k\rangle \\ &\quad + \tfrac{1}{2}\sum_{k=1}^{N} \langle g^l|x_i^m x_j^n \mathbf{x}V_2^k\mathbf{x}|g^k\rangle = \sum_{k=1}^{N} \langle g^l|x_i^m x_j^n V(\mathbf{x})|g^k\rangle; \\ &\quad l = 1, \ldots, N; \quad m+n = 0,1,2; \quad i,j = 1, \ldots, D. \end{aligned} \tag{9}$$

On the right-hand side the potential $V(\mathbf{x})$ of the Hamiltonian is inserted. It is straightforward to calculate the time derivatives of the Gaussian parameters once the linear Eqs. (9) are solved, since the differential equations for the Gaussian parameters can be expressed by $(v_0^k, \mathbf{v}_1^k, V_2^k)$, $k = 1, \ldots, N$, according to their definition in Eq. (8),

$$\dot{A}^k = -2(A^k)^2 - \tfrac{1}{2}V_2^k,$$

$$\dot{\mathbf{q}}^k = \mathbf{p}^k + \mathbf{s}^k,$$

$$\dot{\mathbf{p}}^k = 2\,\mathrm{Re}\,A^k\mathbf{s}^k - \mathrm{Re}\,\mathbf{v}_1^k - \mathrm{Re}\,V_2^k\mathbf{q}^k, \tag{10}$$

$$\dot{\gamma}^k = -v_0^k + i\,\mathrm{tr}\,A^k + \tfrac{1}{2}(\mathbf{p}^k)^2 - \mathbf{v}_1^k\cdot\mathbf{q}^k - \tfrac{1}{2}\mathbf{q}^k V_2^k\mathbf{q}^k + \mathbf{p}^k\cdot\mathbf{s}^k,$$

where $\mathbf{s}^k=(1/2)(\mathrm{Im}\,A^k)^{-1}(\mathrm{Im}\,\mathbf{v}_1^k+\mathrm{Im}\,V_2^k\mathbf{q}^k)$. Numerically, it is more appropriate to introduce two additional $D\times D$ complex matrices B^k and C^k according to $A^k=(1/2)B^k(C^k)^{-1}$, and to integrate the equations of motion

$$\dot{C}^k = B^k,$$

$$\dot{B}^k = -V_2^k C^k, \tag{11}$$

instead of integrating $A^k(t)$ directly, because the oscillating $(A^k(t))^2$ term causes numerical difficulties.[16] For numerical accuracy, it is appropriate to symmetrize the matrix $A^k(t)$ after each time step.

Equation (9) can be abbreviated by $K\mathbf{v}=\mathbf{r}$ when all coefficients $(v_0^k,\mathbf{v}_1^k,V_2^k)$, $k=1,\ldots,N$ are put together into the complex vector $\mathbf{v}$. All inner products in Hilbert space denoted by $\langle .|.\rangle$ are calculated in position space representation. The integrals that build up the components of the matrix K on the left-hand side of Eq. (9) as well as the integrals on the right-hand side can be solved analytically, provided that the potential is of special form, e.g., polynomial, Gaussian, or exponential.

Given some initial wave function, i.e., the initial parameters $\mathbf{z}(t=0)$, the wave function is propagated by integrating the trajectories of the parameters. At every time step, Eq. (9) must be solved for the coefficients $\mathbf{v}$ which are inserted in Eq. (10) to obtain $\dot{\mathbf{z}}$. In the course of integration, depending on how many GWPs are propagated in common, it will sooner or later happen that the matrix K associated with the set of linear Eqs. (9) becomes ill conditioned, or even numerically singular. As a result, the time step of the integration routine becomes extremely small, rendering the method of GWP propagation impracticably slow. In the worst case, further integration or matrix inversion, respectively, can even fail.

III. INEQUALITY CONSTRAINED TDVP

Matrix singularity problems arise from overcrowding the basis set, i.e., from situations where fewer GWPs would be sufficient to represent the wave function. On the other hand, for an accurate approximation of the wave function, it is desirable to have a large number of adjustable parameters. However, there is a discrepancy between the number of GWPs necessary to give accurate results and the maximum number of GWPs that can be propagated using the TDVP without numerical difficulties.[5] As mentioned above, there exist different proposals to overcome this numerical problem, such as a singular value decomposition of the matrix K (Ref. 7) or reducing the number of GWPs when overcrowding takes place.[3,4,9] Also, reducing the variational freedom by freezing the widths[3–5,10] and choosing classical trajectories for the centers of the GWPs (Refs. 2, 6, and 11) have been discussed.

Our approach of regularizing the equations of motion for the parameters is based on minimizing the quantity I in Eq. (1) while certain inequality constraints are applied. The constraints must be chosen in such a way that they prevent the matrix K in Eq. (9) to become ill conditioned. This means that all Gaussian parameters evolve freely according to the TDVP, and the constraints only become active from time to time whenever the unconstrained evolution would drive the parameters in domains where the matrix would be too singular, and are switched off as soon as these "forbidden" domains are left again. Formally speaking, we reduce the space of admissible configurations to regions where the associated matrix K is regular.

To demonstrate the generality of our method we first apply constraints to the general case of an arbitrary trial function $\chi(\mathbf{z}(t))$ whose parameters $\mathbf{z}(t)$ evolve according to Eq. (3). We derive their modified equations of motion which are obtained if the parameters $\mathbf{z}(t)$ are subject to some arbitrary inequality constraints. Then we return to GWPs trial functions (7) and derive the modification of Eq. (9) obtained when the GWP are subject to inequality constraints. Adequate constraints which prevent the matrix from singularity are presented and applied.

Due to real inequality constraints it is convenient to use a real formulation of the equations. Complex quantities are split into their real and imaginary parts, which are denoted by the subscripts r and i, respectively.

A. Inequality constrained TDVP on arbitrary trial functions

Consider an arbitrary trial function $\chi(\mathbf{z}(t))$ and assume a real inequality constraint on the parameters $\mathbf{z}(t)\in\mathbb{C}^{n_p}$ which can be written in the form

$$f(\mathbf{z},\mathbf{z}^*) \equiv f(\mathbf{z}_r,\mathbf{z}_i) \equiv f(\bar{\mathbf{z}}) \geqslant f_{\min}, \tag{12}$$

where the function f is explicitly known. For brevity, the notation $\bar{\mathbf{z}}\equiv(\mathbf{z}_r,\mathbf{z}_i)\in\mathbb{R}^{2n_p}$ will be used.

As long as $f(\mathbf{z}_r,\mathbf{z}_i)>f_{\min}$, all parameters evolve according to Eq. (3) without being affected by the restriction. When $f(\mathbf{z}_r,\mathbf{z}_i)=f_{\min}$ is reached at some point in time t, the constraint becomes active, and we have to demand $\dot{f}(t)\geqslant 0$, otherwise $f(t+\Delta t)$ with some small positive Δt would violate the constraint (12). Therefore, the quantity I of Eq. (1) at fixed $\mathbf{z}$ must be minimized with respect to $\dot{\mathbf{z}}$, where $(\dot{\mathbf{z}}_r,\dot{\mathbf{z}}_i)$ are now subject to the constraint

$$\dot{f} = \frac{\partial f}{\partial \mathbf{z}_r}\cdot\dot{\mathbf{z}}_r + \frac{\partial f}{\partial \mathbf{z}_i}\cdot\dot{\mathbf{z}}_i \equiv \frac{\partial f}{\partial \bar{\mathbf{z}}}\cdot\dot{\bar{\mathbf{z}}} \geqslant 0. \tag{13}$$

In other words the possibly nonlinear constraint (12) on $\mathbf{z}$ has been reduced to the linear constraint (13) on $\dot{\mathbf{z}}$ when $f=f_{\min}$. Then the allowed domain of $(\dot{\mathbf{z}}_r,\dot{\mathbf{z}}_i)$ for searching the minimum of I is no more the whole space $\mathbb{R}^{2n_p}$, but the half-space $\dot{f}\geqslant 0$ linearly restricted by Eq. (13). In general, minimization of a function on a given domain requires two steps; first, to find the local internal minima and, second, to find the local

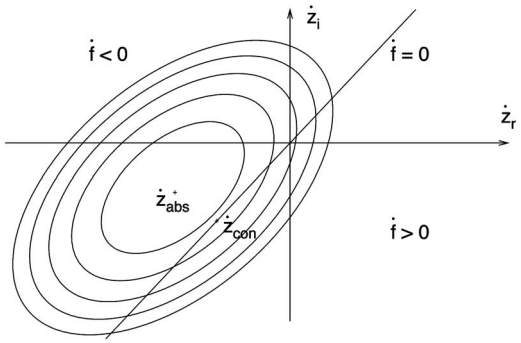

FIG. 1. The ellipses schematically represent isolines of I in Eq. (1) for fixed parameters $\mathbf{z}$. The domain of allowed $\dot{\mathbf{z}}$ for the minimum of I is the full space, when $f>f_{\min}$, and is reduced to the half-space $\dot{f}\geqslant 0$, when $f=f_{\min}$ is reached.

minima on the boundaries. The global minimum in the given domain is obtained by comparison. Here, it is sufficient to search for the minimum of I solely on the boundary of the domain defined by Eq. (13) where the equality sign is fulfilled. That means the inequality (13) may be replaced by the computationally much more feasible constraint

$$\frac{\partial f}{\partial \mathbf{z}_r}\cdot\dot{\mathbf{z}}_r+\frac{\partial f}{\partial \mathbf{z}_i}\cdot\dot{\mathbf{z}}_i\equiv\frac{\partial f}{\partial \bar{\mathbf{z}}}\cdot\dot{\bar{\mathbf{z}}}=0. \tag{14}$$

The reason is that I is a positive definite parabolic function of $\dot{\mathbf{z}}$ whose absolute minimum lies outside the allowed domain by assumption. Since there are no internal minima, I obviously takes its allowed minimum on the boundary of the allowed domain. The constraint is switched off again as soon as the trajectory $\dot{\mathbf{z}}(t)$ of the absolute minimum of I crosses the plane given by Eq. (14) in the $(\dot{\mathbf{z}}_r,\dot{\mathbf{z}}_i)$ space at fixed values of $(\mathbf{z}_r,\mathbf{z}_i)$. Note that arbitrary nonlinear constraints (12) on $\mathbf{z}$ always lead to linear constraints (13) on $\dot{\mathbf{z}}$ leading to a linearly equality constrained quadratic minimization problem, which can directly be solved by a matrix equation as in the unconstrained case (3). The strategy is illustrated in Fig. 1, which shows schematically the elliptical isolines of I for fixed $\mathbf{z}$ as a function of $(\dot{\mathbf{z}}_r,\dot{\mathbf{z}}_i)$. The values of the parameters $\mathbf{z}$ determine the shape and the position of the parabola as well as the slope of the plane $\dot{f}=0$. In Fig. 1, $\dot{\mathbf{z}}_{\text{abs}}$ denotes the absolute minimum of I, obtained from Eq. (3). The plane $\dot{f}=0$ [Eq. (14)] divides the $2n_p$-dimensional $(\dot{\mathbf{z}}_r,\dot{\mathbf{z}}_i)$ space into the two half-spaces $\dot{f}<0$ and $\dot{f}\geqslant 0$. The point $\dot{\mathbf{z}}_{\text{con}}$ is the constrained minimum of I in the half-space $\dot{f}\geqslant 0$, which lies on its boundary, i.e., on the plane $\dot{f}=0$ as explained above.

As long as $f>f_{\min}$, $\dot{\mathbf{z}}_{\text{abs}}$ determines the evolution of the parameters. However, when $f=f_{\min}$ is reached, then $\dot{\mathbf{z}}_{\text{con}}$ is taken for the further integration of the trajectories $\mathbf{z}(t)$ until $\dot{\mathbf{z}}_{\text{abs}}$, driven by the constrained evolution of the parameters, eventually crosses the plane $\dot{f}=0$ from $\dot{f}<0$ to $\dot{f}>0$. At this point, $\dot{\mathbf{z}}_{\text{abs}}$ and $\dot{\mathbf{z}}_{\text{con}}$ coincide and $\dot{\mathbf{z}}_{\text{abs}}$ is taken again for further integration, since $\dot{f}>0$ leads to an increase of $f(t)$ with time, according to the constraint.

For the extension to multiple, say, m active constraints the real scalar valued function $f(\mathbf{z}_r,\mathbf{z}_i)$ is simply replaced by the real vector valued function $\mathbf{f}(\mathbf{z}_r,\mathbf{z}_i)\equiv\mathbf{f}(\bar{\mathbf{z}})=(f_1,\ldots,f_m)\in\mathbb{R}^m$.

Now that the nonholonomic nonlinear inequality constraints (12) on $\mathbf{z}$ are reduced to the holonomic linear equality constraints (14) on $\dot{\mathbf{z}}$ by the constrained TDVP, we can determine the constrained minimum $\dot{\mathbf{z}}_{\text{con}}$ by a standard method such as Lagrangian multipliers. Alternatively, the constrained minimum can also be obtained by elimination of the dependent variational parameters. We prefer the method of Lagrange multipliers due to its generality. The method of Lagrange multipliers yields a compact form of the equations of motion for arbitrary constraints and the conditions for switching off the constraints are obtained with only little additional numerical effort as will be shown below. Both methods however, require a minimization problem with equality constraints. When inequality constraints are applied, the elimination of dependent variational parameters is not possible.

We construct the function

$$L=I+\boldsymbol{\lambda}\bar{M}\dot{\bar{\mathbf{z}}}, \tag{15}$$

with the Lagrangian multipliers $\boldsymbol{\lambda}\in\mathbb{R}^m$ and the real valued $m\times 2n_p$ matrix $\bar{M}=\partial\mathbf{f}/\partial\bar{\mathbf{z}}$. The minimum of I under the constraint (13) is found by $\partial L/\partial\boldsymbol{\omega}=0$, where

$$\boldsymbol{\omega}\equiv\begin{pmatrix}\dot{\mathbf{z}}_r\\ \dot{\mathbf{z}}_i\\ \boldsymbol{\lambda}\end{pmatrix}\equiv\begin{pmatrix}\dot{\bar{\mathbf{z}}}\\ \boldsymbol{\lambda}\end{pmatrix}\in\mathbb{R}^{2n_p+m}.$$

We obtain a set of linear equations

$$\left(\begin{array}{c|c}\bar{K} & \bar{M}^T\\ \hline \bar{M} & 0\end{array}\right)\begin{pmatrix}\dot{\bar{\mathbf{z}}}\\ \boldsymbol{\lambda}\end{pmatrix}=\begin{pmatrix}\bar{\mathbf{h}}\\ 0\end{pmatrix},\quad\text{with }\bar{K}=\begin{pmatrix}K_r & -K_i\\ K_i & K_r\end{pmatrix},$$

$$\bar{\mathbf{h}}=\begin{pmatrix}\mathbf{h}_i\\ -\mathbf{h}_r\end{pmatrix}, \tag{16}$$

where the matrix K and the vector $\mathbf{h}$ are the complex quantities of Eq. (3). If no constraint is active, i.e., $m=0$, then Eq. (16) obviously reduces to the real formulation of Eq. (3). We use a real formulation, i.e., complex quantities are split into their real and imaginary parts, because real constraints such as $f>f_{\min}$ naturally lead to real Lagrangian multipliers.

The constraint (14) is switched off again when $\dot{\mathbf{z}}_{\text{abs}}$ crosses the plane $\dot{f}=0$ from $\dot{f}<0$ to $\dot{f}>0$. Finding this event can be accomplished in two ways. The trivial but computationally expensive way is to calculate not only $\dot{\mathbf{z}}_{\text{con}}$ from Eq. (16), which is needed for integration, but additionally $\dot{\mathbf{z}}_{\text{abs}}$ [from Eq. (3)] after every time step of integration and to check when $\dot{f}|_{\dot{\mathbf{z}}_{\text{abs}}}$ changes its sign. This inefficient procedure would require the solution of a complex $n_p\times n_p$ matrix equation for $\dot{\mathbf{z}}_{\text{abs}}$ and, additionally, the solution of the real $(2n_p+m)\times(2n_p+m)$ matrix equation for $\dot{\mathbf{z}}_{\text{con}}$. However, it is much more efficient to check when λ changes its sign for the special case $m=1$. If more than one constraint is active, m

>1, it is recommended to solve the matrix Eq. (16) by decomposition into two blocks, as indicated by the horizontal line in Eq. (16), namely, into

$$\bar{K}\dot{\bar{\mathbf{z}}} + \bar{M}^T\boldsymbol{\lambda} = \bar{\mathbf{h}}, \tag{17}$$

obtained by the upper part of Eq. (16), and the lower part

$$\bar{M}\dot{\bar{\mathbf{z}}} = 0, \tag{18}$$

which represents the active constraints. The solution for the unknowns $\dot{\bar{\mathbf{z}}}, \boldsymbol{\lambda}$ is obtained by first solving Eq. (17) for $\dot{\bar{\mathbf{z}}}$,

$$\dot{\bar{\mathbf{z}}} = \bar{K}^{-1}\bar{\mathbf{h}} - \bar{K}^{-1}\bar{M}^T\boldsymbol{\lambda}, \tag{19}$$

and inserting it in Eq. (18) in order to eliminate $\dot{\bar{\mathbf{z}}}$. The result is a small $m\times m$ matrix equation for determining $\boldsymbol{\lambda}$,

$$\underbrace{\bar{M}\bar{K}^{-1}\bar{M}^T}_{m\times m}\boldsymbol{\lambda} = \bar{M}\bar{K}^{-1}\bar{\mathbf{h}} \in \mathbb{R}^m. \tag{20}$$

The conditions for switching off any of the active constraints are now contained in the right-hand side of Eq. (20), since

$$\dot{\mathbf{f}}\big|_{\dot{\mathbf{z}}_{\mathrm{abs}}} \equiv \frac{\partial \mathbf{f}}{\partial \bar{\mathbf{z}}}\dot{\bar{\mathbf{z}}}_{\mathrm{abs}} \equiv \bar{M}\dot{\bar{\mathbf{z}}}_{\mathrm{abs}} \equiv \bar{M}\bar{K}^{-1}\bar{\mathbf{h}}, \tag{21}$$

due to the definitions. The ith active constraint $(1\leqslant i\leqslant m)$ is to be switched off when the ith component of $\dot{f}\big|_{\dot{\mathbf{z}}_{\mathrm{abs}}}$ changes its sign from minus to plus.

When we insert the Lagrange multipliers calculated from Eq. (20) in Eq. (19), we obtain $\dot{\mathbf{z}}_{\mathrm{con}}$, needed for propagation. Numerically, the calculation of $\bar{K}^{-1}\bar{\mathbf{h}}$ and $\bar{K}^{-1}\bar{M}^T$ in Eq. (20) requires only one factorization of the large matrix $\bar{K}$. After multiplying with $\bar{M}$ from the left, the small set of linear equations (20) for determining $\boldsymbol{\lambda}$ is obtained. Compared to the factorization of $\bar{K}$, the solution of the $m\times m$ matrix Eq. (20) for the Lagrange multipliers is negligible, since the number of parameters n_p will in general exceed the number of constraints m by far, e.g., in our numerical calculation there is $2n_p=240$ and the number m of simultaneously active constraints is not larger than three.

B. Inequality constrained TDVP applied to GWPs

When GWPs are used as trial function, it is convenient to formulate a set of linear equations for the coefficients $\mathbf{v}=\mathbf{v}_r+i\mathbf{v}_i$ first and then to obtain $\dot{\mathbf{z}}$ from Eq. (10) in a second step, just as was done in Sec. II. For these coefficients $\mathbf{v}_r$ and $\mathbf{v}_i$, summarized by the notation $(\mathbf{v}_r,\mathbf{v}_i)=\bar{\mathbf{v}}$, a similar set of linear equations is obtained. Equations (10), which describe the connection between the time derivatives of the parameters and the coefficients, are written in real formulation, where all complex quantities are split into their real and imaginary parts. We obtain

$$\dot{A}_r^k = -\tfrac{1}{2}V_{2r}^k - 2((A_r^k)^2 - (A_i^k)^2),$$

$$\dot{A}_i^k = -\tfrac{1}{2}V_{2i}^k - 2A_r^kA_i^k - 2A_i^kA_r^k,$$

$$\dot{\mathbf{p}}^k = -\mathbf{v}_{1r}^k - V_{2r}^k\mathbf{q}^k + 2A_r^k\Lambda^k\mathbf{v}_{1i}^k + 2A_r^k\Lambda^kV_{2i}^k\mathbf{q}^k,$$

$$\dot{\mathbf{q}}^k = \Lambda^k\mathbf{v}_{1i}^k + \Lambda^kV_{2i}^k\mathbf{q}^k + \mathbf{p}^k,$$

$$\dot{\gamma}_r^k = -v_{0r}^k - \mathbf{v}_{1r}^k\cdot\mathbf{q}^k - \tfrac{1}{2}\mathbf{q}^kV_{2r}^k\mathbf{q}^k + \mathbf{p}^k\Lambda^k\mathbf{v}_{1i}^k + \mathbf{p}^k\Lambda^kV_{2i}^k\mathbf{q}^k - \mathrm{tr}\,A_i^k + \tfrac{1}{2}(\mathbf{p}^k)^2,$$

$$\dot{\gamma}_i^k = -v_{0i}^k - \mathbf{q}^k\cdot\mathbf{v}_{1i}^k - \tfrac{1}{2}\mathbf{q}^kV_{2i}^k\mathbf{q}^k + \mathrm{tr}\,A_r^k, \tag{22}$$

with $\Lambda^k=\frac{1}{2}(A_i^k)^{-1}$.

Using the notation $\bar{\mathbf{z}}=(A_r^1,A_i^1,\mathbf{p}^1,\mathbf{q}^1,\gamma_r^1,\gamma_i^1,\ldots,A_r^N,A_i^N,\mathbf{p}^N,\mathbf{q}^N,\gamma_r^N,\gamma_i^N)$, the complete set of Eq. (22) for all $k=1,\ldots,N$, which are linear in $(v_0^k,\mathbf{v}_1^k,V_2^k)$, may be written in short form $\dot{\bar{\mathbf{z}}}=\tilde{U}\bar{\mathbf{v}}+\tilde{\mathbf{d}}$. The matrix $\tilde{U}$ is block diagonal with N blocks. Each block consists of those coefficients in Eq. (22) linear in $(v_0^k,\mathbf{v}_1^k,V_2^k)$. The constant terms are absorbed in the vector $\tilde{\mathbf{d}}$. The linear equality constraint (14) for a GWP trial function reads

$$\dot{f} = \sum_{k=1}^{N}\left(\frac{\partial f}{\partial A_r^k}\dot{A}_r^k + \frac{\partial f}{\partial A_i^k}\dot{A}_i^k + \frac{\partial f}{\partial \mathbf{p}^k}\cdot\dot{\mathbf{p}}^k + \frac{\partial f}{\partial \mathbf{q}^k}\cdot\dot{\mathbf{q}}^k + \frac{\partial f}{\partial \gamma_r^k}\dot{\gamma}_r^k + \frac{\partial f}{\partial \gamma_i^k}\dot{\gamma}_i^k\right) = 0, \tag{23}$$

where the notation

$$\frac{\partial f}{\partial A_r^k}\dot{A}_r^k = \sum_{l,j=1}^{D}\frac{\partial f}{\partial (A_r^k)_{lj}}(\dot{A}_r^k)_{lj} \tag{24}$$

is used. Expressing the time derivatives in Eq. (23) by the coefficients $\mathbf{v}_r$ and $\mathbf{v}_i$ using Eq. (22), m arbitrary constraints $[\mathbf{f}=(f_1,\ldots,f_m)\in\mathbb{R}^m]$ imply

$$\dot{\mathbf{f}} = \frac{\partial \mathbf{f}}{\partial \bar{\mathbf{z}}}\tilde{U}\bar{\mathbf{v}} + \frac{\partial \mathbf{f}}{\partial \bar{\mathbf{z}}}\tilde{\mathbf{d}} \equiv \bar{U}\bar{\mathbf{v}} + \bar{\mathbf{d}} = 0, \tag{25}$$

and, hence, a set of linear equations for $(\mathbf{v}_r,\mathbf{v}_i)$ and the Lagrange multipliers $\boldsymbol{\lambda}\in\mathbb{R}^m$ is obtained,

$$\left(\begin{array}{c|c}\bar{K} & \bar{U}^T\\ \hline \bar{U} & 0\end{array}\right)\begin{pmatrix}\bar{\mathbf{v}}\\ \boldsymbol{\lambda}\end{pmatrix} = \begin{pmatrix}\bar{\mathbf{r}}\\ -\bar{\mathbf{d}}\end{pmatrix}, \quad \text{with } \bar{K} = \begin{pmatrix}K_r & -K_i\\ K_i & K_r\end{pmatrix},$$

$$\bar{\mathbf{r}} = \begin{pmatrix}\mathbf{r}_r\\ \mathbf{r}_i\end{pmatrix}. \tag{26}$$

Here, $K=K_r+iK_i$ and the vector $\mathbf{r}=\mathbf{r}_r+i\mathbf{r}_i$ are the matrix and the right-hand side of Eq. (9), respectively.

We now have all equations needed for propagation of coupled GWPs subject to arbitrary constraints (12). Instead of Eq. (9), we solve Eq. (26) for $(\mathbf{v}_r,\mathbf{v}_i)$ (when no constraints are active both sets of equations are equivalent) after each time step. These coefficients are inserted in Eq. (10) [or equivalently in Eq. (22)] to obtain the time derivatives of the Gaussian parameters, which are needed by the integration routine to integrate the next time step.

In order to find convenient constraints, it is necessary to investigate the reasons for the numerical matrix singularity. The generic reasons for an ill conditioned matrix K are twofold. One cause is a strong overlap of neighboring GWPs, and the other cause is widely spread norms of the GWPs. A restriction on the norm of the GWP,

$$g_{\min} \leqslant \|g^k\| \leqslant g_{\max}, \quad k=1,\ldots,N, \tag{27}$$

turns out to be sufficient to regularize the equations of motion. It is, however, more simple and numerically efficient to impose the restrictions

$$f_{\min} \equiv \gamma_{\min} \leqslant f^k(\bar{\mathbf{z}}) = \mathrm{Im}\ \gamma^k \leqslant \gamma_{\max} \equiv f_{\max}, \quad k=1,\ldots,N \tag{28}$$

on the amplitude of the GWP. Both restrictions (27) and (28) are equivalent for frozen GWPs and they are similar even for thawed GWPs (at least for bounded systems where the width of the GWP is bounded by the potential). For the active constraints ($\gamma_i^k=\gamma_{\min}$ or $\gamma_i^k=\gamma_{\max}$), Eq. (14) using Eq. (22) translates into

$$\dot{\gamma}_i^k = -v_{0i}^k - \mathbf{q}^k \cdot \mathbf{v}_{1i}^k - \tfrac{1}{2}\mathbf{q}^k V_{2i}^k \mathbf{q}^k + \mathrm{tr}\, A_r^k = 0. \tag{29}$$

Therefore, in the notation of Eqs. (25) and (26), the entries of $\bar{U}$ are mostly zero except for the terms of Eq. (29) and $\bar{d}=\mathrm{tr}\, A_r^k$. This especially simple case of constraints, where Gaussian parameters are bounded directly, leads to simply temporary freezing these parameters γ_i^k when $\gamma_i^k=\gamma_{\min}$ ($\gamma_i^k=\gamma_{\max}$) is reached. As mentioned above, the equations of motion can, instead of using Lagrange multipliers, be alternatively obtained by elimination of the dependent parameters. The frozen γ_i^k must be simply ignored in the variation. However, additional calculations are then necessary to find the criteria for switching off the constraints.

Should in some cases the restriction on the amplitudes (28) not be adequate, an upper bound on the maximum of the allowed overlap of neighboring GWPs or a lower bound on the least eigenvalue of the matrix may be applied.

IV. NUMERICAL RESULTS

Numerical tests using coupled GWPs were often performed in one dimension, e.g., on the Morse potential.[3–5] Here, we use a two-dimensional nonintegrable potential for testing our method. The Hamiltonian of the system represents the diamagnetic Kepler problem in a 2D rotating (x,z) frame (for review, see, e.g., Refs. 17 and 18). The magnetic field axis is directed along the z axis. The potential in regularized semiparabolic coordinates reads

$$V(\mu,\nu) = \alpha(\mu^2+\nu^2) + \tfrac{1}{8}\beta^2\mu^2\nu^2(\nu^2+\mu^2), \tag{30}$$

with

$$r^2 = x^2+z^2, \quad \mu^2 = r+z, \quad \nu^2 = r-z. \tag{31}$$

The parameters are set to $\alpha=1/2$ and $\beta=1/5$ in our calculations.

The method of free GWP propagation is compared to the method of constrained GWP propagation. The value of the lower bound in Eq. (28) is $\gamma_{\min}=-6.5$, an upper bound was not needed. The comparison is presented in Fig. 2. The trial wave function consists of eight GWPs with the same initial values for both calculations. Solid lines represent results of the free propagation, and dashed lines represent the results of constrained propagation. In Fig. 2(a) the normalization parameter $\gamma_i^k(t)$ is selected and drawn such that it first reaches $\gamma_{\min}=-6.5$ at $t\approx 6.9t_{\mathrm{cl}}$, where t_{cl} is the classical period of small harmonic oscillations around the minimum of the potential. This choice allows for a direct comparison, because the trajectories of both calculations are equal before $\gamma_{\min}$ is reached for the first time by any of the γ^k, and they differ afterwards. Normalization parameters of the other seven GWPs are not plotted but show similar qualitative behavior. In terms of Fig. 1, the trajectories $\gamma_i^k(t)$ in the range of $6.9t_{\mathrm{cl}} \leqslant t \leqslant 7.15t_{\mathrm{cl}}$ are obtained using $\dot{\mathbf{z}}_{\mathrm{abs}}$ for the integration of the solid line and using $\dot{\mathbf{z}}_{\mathrm{con}}$ for the integration of the dashed line. Obviously, the trajectory represented by the dashed line sticks to the value $\gamma_{\min}=-6.5$ until $t\approx 7.15t_{\mathrm{cl}}$, where $\dot{\mathbf{z}}_{\mathrm{abs}}$ crosses the plane $\dot{\gamma}_i^k=0$. This scenario repeats several times as can be seen in the figure. Figure 2(b) compares the step sizes used by the variable step Adams routine to integrate the trajectories. The integration of the unconstrained equations of motion becomes extremely slow around $t\approx 7.1t_{\mathrm{cl}}$, and later on again for several times where the step sizes become tiny. Obviously, there is a strong correlation between very low values of γ_i^k in panel (a) and extremely small step sizes in panel (b) for unconstrained propagation. In regions where the free propagation is very slow, the step sizes for the constrained propagation are about two to four orders of magnitude larger, resulting in a much faster integration.

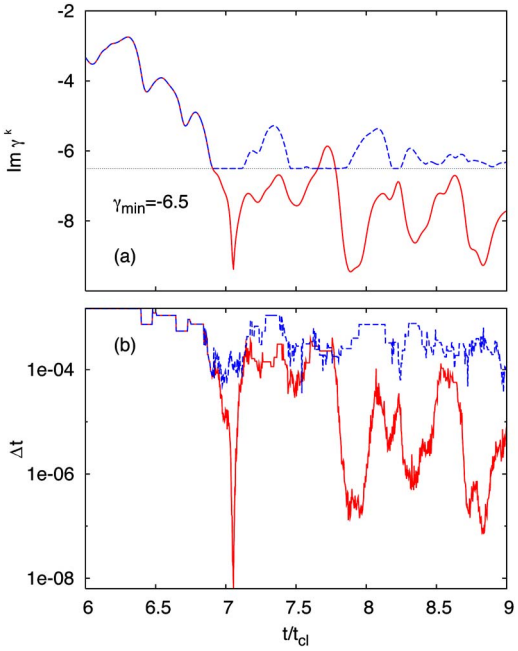

FIG. 2. (Color online) Comparison between free and constrained GWP propagations of the same initial wave function consisting of a superposition of eight GWPs in the 2D diamagnetic Kepler problem: (a) Normalization parameter that first reaches $\gamma_{\min}$, and (b) comparison of the step sizes Δt used by the integrator (variable step Adams method). Solid lines denote free propagation, and dashed lines denote propagation with the constraints $\gamma^k \geqslant \gamma_{\min}=-6.5$, $k=1,\ldots,N$. In both calculations the same error tolerances were used.

The magnitude of I at its minimum is a measure of the accuracy of the variational approximation.[19,20] Therefore, a comparison of the minima $I|_{\dot{\mathbf{z}}_{\mathrm{abs}}}$ and $I|_{\dot{\mathbf{z}}_{\mathrm{con}}}$ allows for an estimate of the loss of accuracy introduced by the constraints. A comparison of the minima shows that $I|_{\dot{\mathbf{z}}_{\mathrm{con}}}$ is slightly increased at $t\approx 6.9t_{\mathrm{cl}}$ with respect to $I|_{\dot{\mathbf{z}}_{\mathrm{abs}}}$, but at

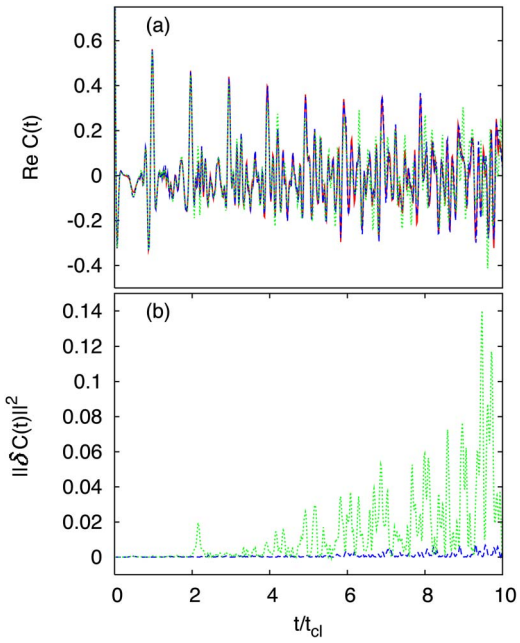

FIG. 3. (Color online) (a) Real part of the autocorrelation function. The initial wave function for the 2D diamagnetic Kepler problem is a superposition of 20 GWPs. Variational propagation with the constraints $\gamma^k \geqslant -6.5$ (dashed line) is compared with numerically exact calculations (solid line) and with frozen GWP propagation (dotted line). The results of the constrained calculation and the numerically exact calculation practically coincide, and nearly no deviation is visible. (b) Deviations of the autocorrelation functions calculated by constrained GWP (dashed line) and by frozen GWP (dotted line) from the exact one.

later times, one approximation is about as good as the other in the average, although a poorer approximation of the constrained wave function to the exact one would be expected. However, it has been shown that the approximate wave function determined by TDVP is not always the "best" possible approximation of the trial function to the exact wave function.[20] There might be regions on the manifold of the trial function that are closer to the exact wave function than the function determined variationally, especially when the manifold has a large curvature and long time intervals are considered. This fact, together with the insensitivity of the wave function to small variations of the parameters in some directions in case of a singular matrix, may explain the behavior of only temporary slight loss of accuracy introduced by the constraints. The insensitivity of the trial wave function to the constraints can also be deduced from the autocorrelation functions $C(t)=\langle\chi(t=0)|\chi(t)\rangle$ obtained by both methods since they almost coincide and no deviation from each other could be seen in any figure.

To demonstrate the accuracy of the constrained GWP method, a superposition of 20 GWPs all having the same width and zero momenta, equally distributed on an equidistant grid, was used as the initial wave packet. This initial wave packet was propagated by three different methods. The real parts of the resulting autocorrelation functions are plotted in Fig. 3(a). The imaginary parts, not shown in the figure, exhibit similar behavior. For reference the numerically exact propagation was performed by the split operator method[21] (solid line). The result of our constrained ($\gamma^k \geqslant 6.5$) GWP propagation (dashed line) is mostly very accurate and nearly no deviation from the exact solution is visible for many classical periods. By contrast, the result obtained from a frozen Gaussian propagation (dotted line) turns out to be much more inaccurate. This becomes particularly apparent in Fig. 3(b), where the deviation between the exact time signal and the time signals obtained from constrained (dashed) and from frozen width (dotted) propagations is plotted. For short times, both methods are very accurate and nearly no deviation between the time signals is visible. With increasing time, however, the accuracy of the frozen width calculation is lost much faster than that of the constrained propagation. This is not completely unexpected since the constrained trial function still has more free variational parameters than the frozen GWP method and, therefore, the constrained calculation is slower. Note that an unconstrained propagation of these 20 GWPs with variable widths according to the TDVP would not be possible. With the propagated wave packet at hand, it is straightforward to obtain e.g., the eigenvalues of the Hamiltonian by Fourier transform or harmonic inversion (for a review see, e.g., Ref. 22) of the autocorrelation function or to extract eigenfunctions of the system (e.g., Ref. 23).

V. SUMMARY

A novel method to overcome the matrix singularity problem in the variational Gaussian wave packet method has been proposed. The method is based on applying nonholonomic inequality constraints on the motion of the GWPs. The constraints must be chosen to prevent the matrix from becoming singular. From the inequality constrained TDVP, a simple matrix equation for the time derivatives of the parameters is obtained just as in unconstrained TDVP. The method is, in fact, applicable for arbitrary trial functions and inequality constraints. For the GWP trial functions, we found it sufficient in most cases to apply simple bounds on the normalization parameters to regularize the matrix and to obtain well behaved equations of motion, rendering the integration orders of magnitude faster. The loss of accuracy of the method caused by the constraints is found to be negligible for sufficiently many GWPs. The method allows for the propagation of a large number of coupled GWPs, as compared to the unconstrained GWP propagation, and guarantees accurate results within reasonable time. Our method for time propagation of constrained coupled Gaussian wave packets presented in this article will be very powerful in a large variety of future applications to overcome the problems with ill conditioned and stuck differential equations.

[1] E. J. Heller, J. Chem. Phys. **62**, 1544 (1975).
[2] E. J. Heller, J. Chem. Phys. **64**, 63 (1976).
[3] S.-I. Sawada, R. Heather, B. Jackson, and H. Metiu, J. Chem. Phys. **83**, 3009 (1985).
[4] R. Heather and H. Metiu, J. Chem. Phys. **84**, 3250 (1986).
[5] F. Hansen, N. E. Henriksen, and G. D. Billing, J. Chem. Phys. **90**, 3060 (1989).
[6] R. T. Skodje and D. G. Truhlar, J. Chem. Phys. **80**, 3123 (1984).
[7] K. G. Kay, Chem. Phys. **137**, 165 (1989).
[8] T. Fabčič, J. Main, and G. Wunner, Nonlinear Phenom. Complex Syst. (Minsk, Belarus) **10**, 86 (2007).
[9] I. Horenko, M. Weiser, B. Schmidt, and C. Schütte, J. Chem. Phys. **120**, 8913 (2004).
[10] E. J. Heller, J. Chem. Phys. **75**, 2923 (1981).
[11] J. Zoppe, M. L. Parkinson, and M. Messina, Chem. Phys. Lett. **407**, 308

(2005).
[12] P. A. M. Dirac, Proc. Cambridge Philos. Soc. **26**, 376 (1930).
[13] J. Frenkel, *Wave Mechanics, Advanced General Theory* (Clarendon, Oxford, 1934).
[14] A. D. McLachlan, Mol. Phys. **8**, 39 (1964).
[15] P. Kramer and M. Saraceno, *Geometry of the Time-Dependent Variational Principle in Quantum Mechanics*, Lecture Notes in Physics 140 (Springer, Berlin, 1981).
[16] E. J. Heller, J. Chem. Phys. **65**, 4979 (1976).
[17] H. Friedrich and D. Wintgen, Phys. Rep. **183**, 37 (1989).
[18] H. Hasegawa, M. Robnik, and G. Wunner, Prog. Theor. Phys. Suppl. **98**, 198 (1989).
[19] A. Raab, Chem. Phys. Lett. **319**, 674 (2000).
[20] C. Lubich, Math. Comput. **74**, 765 (2005).
[21] M. D. Feit, J. A. Fleck, Jr., and A. Steiger, J. Comput. Phys. **47**, 412 (1982).
[22] J. Main, Phys. Rep. **316**, 233 (1999).
[23] J. R. Reimers and E. J. Heller, J. Phys. A **19**, 2559 (1986).